Neuroradiology (1992) 34: 135–140

Neuro radiology

Experimental focal cerebral ischaemia assessed with IVIM*-MRI in the acute phase at 0.5 tesla

I. Berry[1], M. Gigaud[2], and C. Manelfe[1]

[1] Neuroradiology and MRI unit and [2] Neurosurgery, CHU Purpan, Toulouse, France

Received: 12 September 1991

Summary. Intravoxel incoherent motion (IVIM*)-MRI has been performed on a clinical system at 0.5 tesla with a b gradient factor of 100 s/mm^2, in a feline focal model of cerebral ischaemia. Images were obtained in 26 cats from less than 1 hour and up to 7–12 hours after stroke. The apparent diffusion coefficient (ADC) was decreased at the site of injury when compared to the contralateral normal side, by 30 % in the first, 33 % in 1–2 h and 27 % in 2–4 h; it increased at 7–12 h, when vasogenic oedema occurred. IVIM*-MRI demonstrated early changes, due to cytotoxic oedema, during the acute phase of cerebral ischaemia to which conventional T2-weighted spin-echo imaging was not sensitive.

Key words: Magnetic resonance imaging – Experimental brain ischemia – Brain oedema – Diffusion

The term intravoxel incoherent motion (IVIM*) was recently introduced by Le Bihan et al [1] to describe microscopic movements of molecules within a voxel during the echo time of an image acquisition. These include Brownian molecular motion, capillary perfusion and nonuniform slow flow. Like proton density and T1 and T2 relaxation times, flow influences spin-echo signal intensity; it does so by producing phase shifts, giving rise to signal loss. Although this is macroscopically perceived for larger scale motions than IVIM*, this process may also visibly influence signal intensity when its phase effects are enhanced by application of additional field gradient. To further improve visualisation of IVIM*, the contribution of the immobile or coherently moving spins may be eliminated by dividing the standard image by the gradient-sensitized one, thereby producing a purely IVIM*-weighted image. Quantification of IVIM* is needed to extend the concept of "diffusion coefficient" to an "apparent diffusion coefficient" (ADC) and to take into consideration the specific in vivo aspects such as perfusion, or restriction of molecular diffusion by cell structure.

Cerebral ischaemia produces an almost immediate neurological deficit. Permanent infarction has delayed effects depending on the duration and severity of the reduction of blood flow. Part of the ischaemic territory, such as the so-called ischaemic penumbra, may remain viable [2]. Alleviation of ischaemia will therefore reverse the lesion in the penumbra, but may aggravate the condition of the already infarcted tissue. To date no investigation has assessed the reversibility of an ischaemic insult, and moreover no high resolution imaging technique can show very early ischaemia noninvasively. Brain ischaemia induces oedema, initially cytotoxic and subsequently vasogenic which, during the first few hours, is not reliably shown on conventional T2-weighted spin-echo MRI [3]. Since IVIM*-MRI reflects capillary perfusion and Brownian motion, it is thought to be able to depict the early stages of brain ischaemia. In addition, it is hypothesised that IVIM*-MRI may be sensitive to the build up of oedema. A model of focal cerebral ischaemia which allows for signal intensities to be compared on the same MR section, has been used to test this hypothesis. Following preliminary work using standard clinical equipment which showed a decrease of ADC in the early stages of brain ischaemia [4], the method was refined to elucidate the mechanism underlying the changes on imaging with the same feline model [5–8], other models of stroke [9–10], or other experimental designs [11, 12]. This required much stronger gradient pulses, usually achieved with shielded gradient coils on experimental systems. The developments of the technique were subsequently very impressive as it could separate IVIM* effects related to diffusion and to perfusion [13–15]. Echoplanar imaging enhanced the potential of IVIM*-MRI further, since it allowed major reduction of acquisition time and studies with several b gradient factors, which permit more accurate in vivo measurements of diffusion coefficients and perfusion factors [16]. The scope of diffusion/perfusion imaging is currently wide, with many research applications [17–20]. This work reports the use of IVIM*-MRI performed on standard clinical equipment at 0.5 tesla to assess the initial and delayed changes following the onset of experimental focal cerebral ischaemia on a series of cats followed for 7–12 hours.

Methods

Animals

Adult cats (2.5–4.2 kg) were used for this study. Anaesthesia was induced with an intramuscular injection of ketamine (50 mg/kg), and maintained in the operated animals with an intravenous infusion of ketamine (10 mg/kg/20 min during surgery, then 2 mg/kg/hour during imaging) through a femoral venous catheter. Thoracic ECG electrodes were in place.

Ten control animals were imaged in the very early phase, after no more than 1 h of anaesthesia. Six were re-imaged after 1–2 h and 7–12 h anaesthesia. These control animals were allowed to recover for at least a week.

Twenty-six animals underwent right middle cerebral artery occlusion (MCAO) through the transorbital approach. Surgical procedure included right orbital exenteration, trepanation above and lateral to the optic canal, opening of the dura mater, bipolar coagulation of the middle cerebral artery proximal to the lenticulostriate branches and division of the coagulated artery to ensure complete interruption of the blood stream.

Images were acquired during the first h (26 cats) and after 1–2 h (26 cats), 2–4 h (19 cats) and 7–12 h (16 cats) of brain ischaemia. The animals were sacrificed with intravenous injection of T61. The brains were removed and frozen. Six animals were sacrificed in the magnet, and IVIM*-MRI was obtained immediately pre- and postmortem 2–4 h after the stroke in 3 cases and following 12 hours in the other 3.

MRI

MRI was performed at 0.5 tesla. A mask-shaped orbit surface coil was positioned on the head of the cats, which were in the prone position. T2-weighted images (TR 1000 ms, TE 140 ms, 7 mm sections, FOV 140 × 140 mm^2) were obtained at all times as part of the IVIM*-MRI acquisition protocol. If the imaging procedure was interrupted early (after 2–4 h of stroke), a bolus injection of 1 mmol/kg dysprosium-DOTA was used [21].

IVIM*-MRI included the use of twin spin-echo sequences acquired with and without the IVIM* gradients. Three coronal IVIM*-MR images (TR cardiac gated with a refractory period of 1000 ms, TE 140 ms, 2 excitations, 7 mm sections, 1 mm gap, FOV 140 × 140 mm^2, data matrix size 256 × 256, pixel 0.30 mm^2) were acquired with IVIM* gradient pulse duration of 40 ms in the read-out direction, a gradient separation of 30 ms (diffusion time 57 ms) and gradient strength of 0.35 G/cm resulting in gradient b values of 100 s/mm^2. The vertical direction was sensitised for coronal slices. The central slice was reproducibly positioned at the level of the pituitary gland. Signal intensity Io and I1 of both raw images as computed pixel by pixel according to the formula ADC (mm^2/s) = ln (Io/I1)/100 to obtain a third, calculated IVIM* image [1].

Region-of-interest (ROI) image analysis was carried out on both raw images; circular ROI (1.36 mm in radius, 20 pixels each) were placed with an interactive cursor in the lesion (in the cortex or, if this was not injured, in the basal ganglia) on the ischaemic side and in the same area on the opposite side. The mean ADC of the ROI was calculated from the above formula. A correction was introduced for discrepancy in image size produced by eddy currents. The Wilcoxon signed rank sum test and the Mann-Whitney U test respectively were used for analysis of paired and unpaired data. Significance level was fixed at $P < 0.05$.

Results

All operated animals developed ischaemia. This was confirmed by T2-weighted images at 7–12 h, which showed oedema as hyperintensity in the damaged right middle cerebral artery territory, which included the cortex and basal ganglia (Fig. 1c, 3a) Occasionally only the deep territory of the middle cerebral artery was damaged, and hyperintensity was restricted to the head of the caudate nucleus on the coronal T2-weighted images (Fig. 2c). When late T2-weighted images were not acquired confirmation of the ischaemia was by the the lack of fall of signal at the injury site following a bolus of the paramagnetic contrast agent dysprosium-DOTA.

An ADC of $3.18 \pm 0.35 \times 10^{-3}$ mm^2/s (n = 5) was calculated from the images of a water sample tube using the same imaging protocol as in the cats.

Table 1 shows the time-course of the ADC of grey matter of controls and MCAO animals. The ADC in the controls and in the normal contralateral grey matter of operated animals as statistically identical at all times of observation. The ADC value of the control animals' cortex was $1.94 \pm 0.28 \times 10^{-3}$ mm^2/s within 1 h of anaesthesia; it decreased slightly but significantly (p = 0.014) to $1.70 \pm 0.30 \times 10^{-3}$ mm^2/s following 7 h of anaesthesia. The

Table 1. Changes in apparent diffusion coefficient (ADC, 10^{-3} mm^2/s, means ± s. d.) with time in cats with occluded middle cerebral arteries (MCAO) and controls

Time of observation / Regions	0–1 h	1–2 h	2–4 h	7–12 h
MCAO injury	N = 26: 1.42 ± 0.63	N = 26: 1.32 ± 0.40	N = 19: 1.20 ± 0.32	N = 16: 1.97 ± 0.39
	↕ $P < 0.001$	↕ $P < 0.001$	↕ $P < 0.003$	↕ $P < 0.001$
Contralateral	N = 26: 2.02 ± 0.44	N = 26: 1.96 ± 0.46	N = 19: 1.64 ± 0.41	N = 16: 1.45 ± 0.42
Control	N = 10: 1.94 ± 0.28	N = 6: 1.98 ± 0.30		N = 6: 1.70 ± 0.30

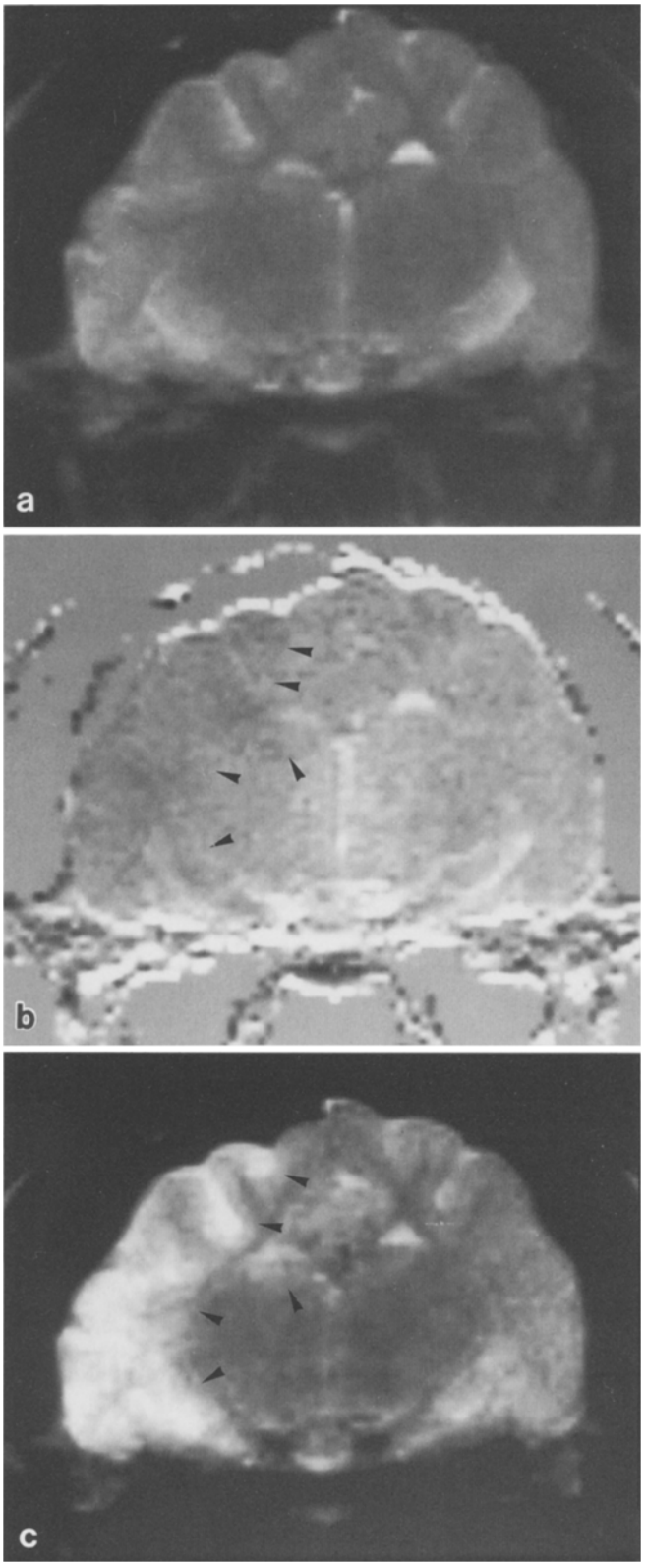

Fig. 1. **a** Coronal T2-weighted image of cat brain within 1 hour of right MCAO. No lesion is seen in the right middle cerebral artery territory. **b** Simultaneous IVIM*-MRI reveals low signal intensity due to decrease in ADC in the right cortex, internal capsule and basal ganglia *(arrows)*. **c** T2-weighted image obtained later shows oedema as high signal intensity in the same locations *(arrows)*

ADC of the normal contralateral hemisphere also decreased with increasing duration of anaesthesia. In the first hour of acute MCAO T2-weighted MRI was negative or equivocal while IVIM*-MRI sometimes exhibited low signal intensity due to decreased ADC in the damaged territories (Fig. 1). In all cases a decrease in ADC, leading to a reduction in signal intensity on IVIM*-MRI preceded visualisation of signal intensity enhancement on T2-weighted images (Fig. 2). During the first hour of ischaemia ADC is decreased by 30 % on the affected side, when compared to its fellow. With time, the relative differences in ADC of ischaemic and contralateral regions remained stable (– 33 % at 1–2 h and – 27 % at 2–4 h), although ADC decreased further on both sides.

After longer periods of ischaemia (7–12 h), while T2-weighted imaging consistently showed the build up of oedema, indicated by high signal intensity, ADC increased (Fig. 3).

Pre- and postmortem images, immediately before and after sacrifice showed a similar pattern of contrast between the damaged and contralateral hemispheres. At 2–4 h after MCA occlusion the postmortem ADC decreased by 30–58 % on the normal side and by 27–35 % on the affected side. After 7–12 h it decreased by 22–36 % on the normal side and by 0.7–2.7 % on the injured side.

Discussion

IVIM*-MRI reveals earlier changes in ischaemic tissues than conventional T2-weighted MRI; this could be important if a noninvasive diagnostic technique which might be used to study the extent of the injury in the early phases of ischaemia were required. If a prognostic value could be confirmed the technique would be clinically beneficial. Indeed, if accurate imaging of the consequences of brain ischaemia were possible, an pathophysiological index of the reversibility of lesions seen in the emergency setting would be established, which could be of importance, since new fibrinolytic medications have been the subject of recent therapeutic trials in the acute phase [22].

We found the ADC of a sample tube containing water to be 35 % higher than expected [1], due possibly to mechanical vibration of the magnet and/or gradient system. Errors related to motion are also possible: although large movement were controlled by anaesthetic monitoring, small movements might have occurred occasionally, because the animals were not paralysed. Since the gradient-sensitised acquisitions are highly sensitive to motion, any movement results in additional amplitude attenuation, artefactually increasing the ADC. Consequently, the absolute values of ADC might all be slightly elevated in our experiments and should thus be treated with caution.

Brain pulsations related to blood and CSF flow increase ADC. Their coherence in time should be ensured by cardiac gating, but any instability in heart rate procedures variable saturation effects in the longitudinal magnetisation between successive cycles, inducing artifacts because the TR is not so long as compared to the T1 values of the imaged tissues. This prompted Le Bihan et al. [11] to use a TR of 5 s at 4.7 tesla to perform more accurate

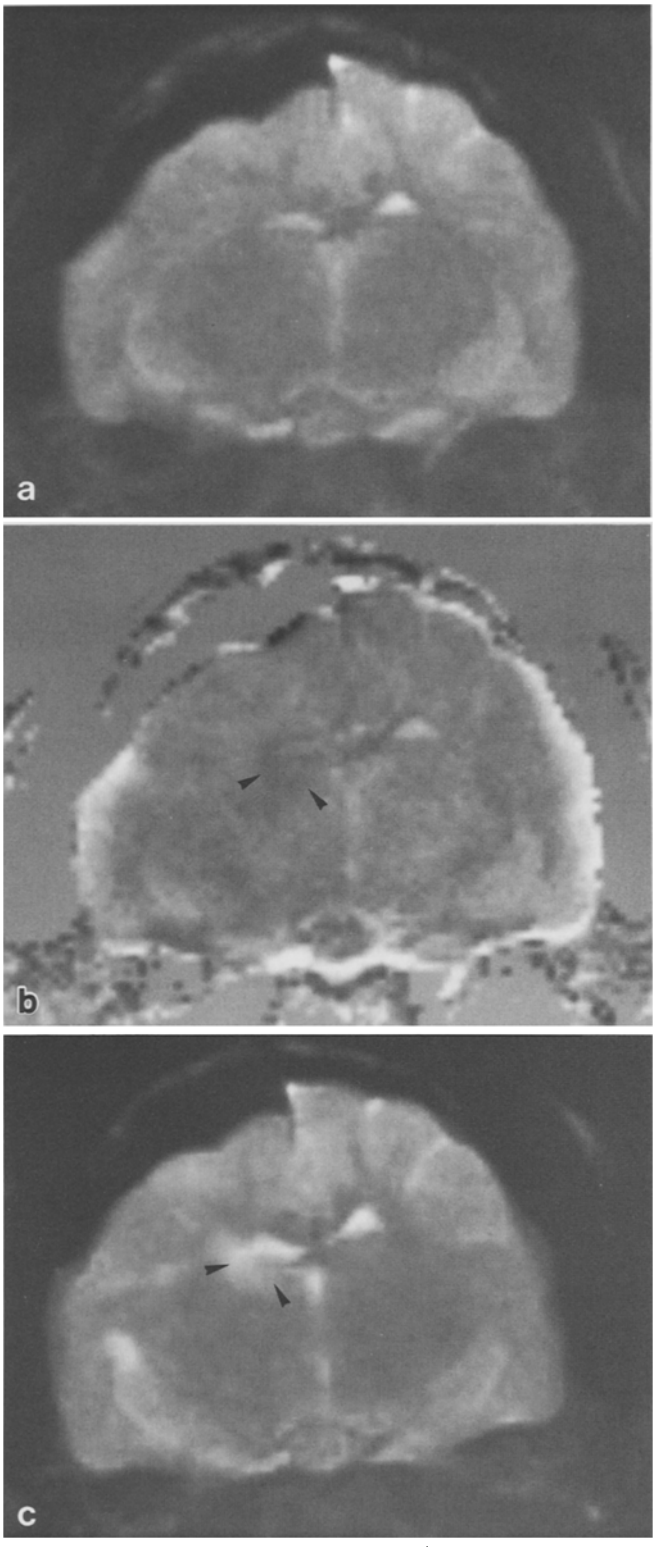

Fig. 2. **a** Coronal T2-weighted image of cat brain 3.5 h after right MCAO; no alteration of signal intensity is observed. **b** IVIM*-MRI performed simultaneously reveals an low signal corresponding to low ADC in the head of the right caudate nucleus *(arrows)*. **c** T2-weighted image 11.5 h following the induction of stroke confirms the presence of a caudate nucleus lesion, in the central territory of the right middle cerebral artery, where oedema has developed *(arrows)*

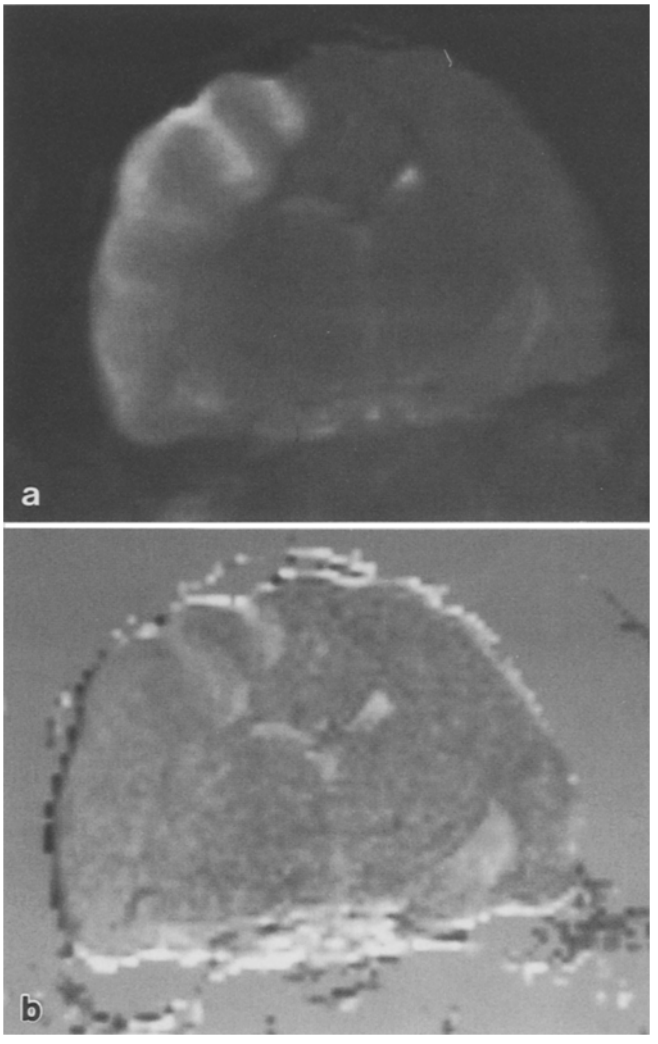

Fig. 3. **a** T2-weighted coronal image of cat brain 10.5 h after right MCAO: note the extent of oedema. **b** IVIM*-MRI shows high signal intensity indicated to elevated ADC, in the same territory

ADC measurements in the normal cat brain, but this prolongs the acquisition time to an extent incompatible with the observation of in vivo processes. Therefore, the observed decrease in ADC of our postmortem images is consistent with their being degraded by pulsation artifacts as well as microcirculatory effects. These are part of the IVIM* and are included in the ADC when studied with a low b gradient factor such as ours (100 s/mm^2) [13]. The incoherent flow effects are eliminated at higher b values, explaining why a diffusion coefficient as low as 0.91×10^{-3} mm^2/s is found for grey mater with b = 1413 s/mm^2 [5].

Pathophysiological explanation of the changes we observed in ADC seen in cerebral injury is difficult since the weak IVIM* gradients do not allow separation of diffusion and perfusion phenomena. The early phases of ischaemia, accompanied by decreased ADC, could be due to a decrease in diffusion and/or perfusion. It has been shown that cerebral blood flow measured by SPECT and ADC with a b gradient factor of 100 s/mm^2 did not correlate in the brain parenchyma of normal volunteers [3]. Therefore the observed data relate not only to the hy-

poperfusion expected in ischaemic tissues but also to a decrease in Brownian movement (diffusion). This suggestion is supported by the results of the San Francisco group, who demonstrated signal intensity changes corresponding to decreased diffusion in the same model at 2.0 tesla, with the use of a much higher b gradient factor (1413 s/mm^2), thus weighting the images only with diffusion, without any influence from perfusion [5–7]. This finding was confirmed by Moonen et al. [8], using the same stroke model, in a rat focal ischaemia model [9, 10] and in focal injury induced with kainic acid [12].

Several mechanisms have been proposed to explain the decreased ADC in the damaged region. 1) The ischaemia imapirs the action of sodium/potassium-ATPase, the membrane enzyme actively transporting sodium out of the cells, into the extracellular space. During ischaemia, sodium accumulates with in the cells and water follows osmotically, creating cytotoxic oedema at the expense of the extracellular space. Water molecules are therefore confined in cells which are smaller (about 10 μm) than the root-mean-square path length of proton diffusion, which has been calculated to be 14–16 μm with an experiment using 33 ms diffusion time [5]. In our conditions, diffusion time is 57 ms and the root-mean-square path length of proton diffusion is 19 μm so that hindrance to increased intracellular water might apply a fortiori. Furthermore experiments with various diffusion times in the same cat model confirmed the thesis of restricted diffusion of intracellular water [8]. 2) Microscopic brain pulsations may be limited inside the damaged tissue, particularly when mass effect is significant. 3) Knight et al. [10] mentioned the possibility of increased magnetic susceptibility-induced field gradient in ischaemic tissue because of reduced tissue oxygenation. 4) Cooling of hypoperfused tissue may cause alterations in ADC, which is highly temperature-dependent (2.4 %/°C [24]).

As mentioned earlier, microcirculation influences ADC in our experimental conditions and hypoperfusion of ischaemic tissue may also contribute to the observed decreased in ADC. The postmortem demonstration of a larger reduction in ADC in the normal hemisphere than on the damaged side may be explained by low residual perfusion on the side of the lesion. Nevertheless, an alternative interpretation may involve the effect of death on brain pulsations which may be already decreased at the site of injury due to mass effect.

An increase in Brownian motion may explain the tendency of ADC of increase in the later stages of cerebral ischaemia, when vasogenic odema is consistently present macroscopically. Movement of water molecules may less restricted since vasogenic oedema involves disruption of cell membranes and an increase in extracellular water. Additional supportive evidence comes from the studies by Knight et al. [10] who showed an increase in the diffusion coefficient of water toward control values between 24 and 48 hours after focal ischaemia in the rat. Similarly, King et al. [11] found increased ADC in the chronic stage of kainic acid brain lesions [11].

The decrease in ADC in the normal hemisphere is certainly related to prolonged anaesthesia. Reduced heart rate and arterial blood pressure, both of which decrease brain pulsation and, to a certain extent, perfusion (although the brain is spared), may explain the progressive decrease in ADC. Decrease in body temperature is also possible, as well as poor oxygenation, since the cats breathed spontaneously throughout the experiment.

This study using a 0.5 tesla clinical system and low b gradient factor to sensitize MRI to IVIM* shows changes in the initial phase of ischaemia, whereas conventional T2-weighted spin-echo imaging does not; these changes are less pronounced than in studies with larger sensitizing gradients. The pathophysiological interpretation is limited by the coexistence of diffusion and perfusion effects, which are not separated in these experimental conditions. Nevertheless, the demonstration of changes induced by stroke, possible using simple clinical equipment, offers functional data which complement the new morphological information given by MRI.

Acknowledgements. Denis LeBihan for helpful advice; A. Aria Tzika, for review of the manuscript; General Electric-CGR (Buc, France), for experimental implementation of the IVIM* software and INSERM (grant 889001), Conseil Régional Midi-Pyrénées and Université Paul Sabatier for financial support

References

1. Le Bihan D, Breton E, Lallemand D, Grenier P, Cabanis E, Laval-Jeantet M (1986) MR imaging of intravoxel incoherent motions: application to diffusion and perfusion in neurologic disorders. Radiology 161: 401–407
2. Astrup J, Siesjö, Symon L (1981) Thresholds in cerebral ischemia. The ischemic penumbra. Stroke 12: 723–725
3. Brant-Zawadzki M, Pereira B, Weinstein P, Moore S, Kucharczyk W, Berry I, MacNamara M, Derugin N (1986) MR imaging of acute experimental ischemia in cats. AJNR 7: 7–11
4. Berry I, Manelfe C, Gigaud M, Breuille P (1988) IVIM*-MRI in experimental acute cerebral ischemia. Soc Magn Reson Med San Francisco (CA), pp 158
5. Moseley ME, Cohen Y, Mintorovitch J, Chileuitt L, Shimizu H, Kucharczyk J, Wendland MF, Weinstein PR (1990) Early detection of regional cerebral ischemia in cats: comparison of diffusion- and T2-weighted MRI and spectroscopy. Mag Res Med 14: 330–346
6. Moseley ME, Kucharczyk J, Mintorovitch J, Cohen Y, Kurhanewicz J, Derugin N, Asgari H, Norman D (1990) Diffusion-weighted MR imaging of acute stroke: correlation with T2-weighted and magnetic susceptibility-enhanced MR imaging in cats. AJNR 11: 423–429
7. Kucharczyk J, Mintorovitch J, Asgari HS, Moseley M (1991) Diffusion/perfusion MR imaging of acute cerebral ischemia. Mag Res Med 19: 311–315
8. Moonen CTW, Pekar J, De Vleeschouwer MHM, Van Gelderen P, Van Zijl PCM, Despres D (1991) Restricted and anisotropic displacement of water in healthy cat brain and in stroke studied by NMR diffusion imaging. Mag Res Med 19: 327–332
9. Mintorovitch J, Moseley ME, Chileuitt L, Shimizu H, Coyen Y, Weinstein PR (1991) Comparison of diffusion- and T2-weighted MRI for the early detection of cerebral ischemia and reperfusion in rats. Mag Res Med 18: 39–50
10. Knight RA, Ordidge RJ, Helpern JA, Chopp M, Rodoloski LC, Peck D (1991) Temporal evolution of ischemic damage in rat brain measured by proton nuclear magnetic resonance imaging. Stroke 22: 802–808
11. Le Bihan D, Moonen CTW, Van Zijl PCM, Pekar J, Despres D (1991) Measuring random microscopic motion of water in tissues with MR imaging: a cat brain study. J Comput Assist Tomogr 15: 19–25

12. King MD, Van Bruggen N, Ahier RG, Cremer JE, Hajnal JV, Williams SR, Doran M (1991) Diffusion-weighted imaging of kainic acid lesions in the rat brain. Mag Res Med 20: 158–168
13. Le Bihan D, Breton E, Lallemand D, Aubin ML, Vignaud J, Laval-Jeantet M (1988) Separation of diffusion and perusion in intravoxel incoherent motion MR Imaging. Radiology 168: 497–505
14. Dixon WR (1988) Separation of diffusion and perfusion in intravoxel incoherent motion MR imaging: a modest proposal with tremendous potential. Radiology 168: 566–567
15. Le Bihan D (1990) Magnetic resonance imaging of perfusion. Mag Res Med 14: 283–292
16. Turner R, Le Bihan D, Maier J, Vavrek R, Hedges LK, Pekar J (1990) Echo-planar imaging of intravoxel incoherent motion. Radiology 177: 407–414
17. Le Bihan D (1990) Diffusion/perfusion MR imaging of the brain: from structure to function. Radiology 177: 328–329
18. Moonen CTW, Van Zijl PCM, Franck JA, Le Bihan D, Becker ED (1990) Functional magnetic resonance imaging in medicine and physiology. Science 250: 53–61
19. Le Bihan D, Turner R, Moonen CTW, Pekar J (1991) Imaging of diffusion and microcirculation with gradient sensitization: design, strategy, and significance. J Magn Res Imag 1: 7–28
20. Moseley ME, Wendland MF, Kucharczyk J (1991) Magnetic resonance imaging of diffusion and perfusion. Top Magn Reson Imaging 3: 50–67
21. Berry I, Manelfe C, Celsis P, Marc-Vergnes JP (1989) Correlation between intravoxel incoherent motions-MRI (IVIM*-MRI) and cerebral blood flow (CBF) as measured by single photon emission computed tomography (SPECT). Soc Magn Reson Med, Amsterdam, pp 10
22. Del Zoppo GJ (1988) Thrombolytic therapy in cerebrovascular disease. Stroke 23: 7–12
23. Berry I, Chambon C, Gigaud M, Derache V, Manelfe C (1990) Early depiction of brain ischemia with MRI and Dysprosium-DOTA injection. XIV Symposium Neuroradiologicum, London
24. Le Bihan D, Delannoy J, Levin RL (1989) Temperature mapping with MRI imaging of molecular diffusion: application to hyperthermia. Radiology 17: 853–857

I. Berry, M.D., Ph.D.
Neuroradiology and MRI Unit
CHU Purpan Place du Dr. Baylac
F-31 059 Toulouse
France